Investigation of collisions of electrons with noble gas atoms at thermal and subthermal energies by electron cyclotron resonance spectroscopy

K. S. Golovanivskiĭ and A. P. Kabilan

Patrice Lumumba Friendship of Nations University, Moscow
(Submitted 20 November 20 1980)
Zh. Eksp. Teor. Fiz. **80**, 2210–2220 (June 1981)

Electron cyclotron resonance spectroscopy consists in numerical simulation of experimental resonance curves. The simulation procedure involves three-parameter fitting of the O'Malley formulas for the expansion of the scattering phases at low energies so that the corresponding energy dependences of the momentum transfer cross sections and the electron distribution functions ensure the agreement between the experimental and simulated electron cyclotron resonance spectra with the required precision. The values of the cross sections and scattering phases are obtained in the form of continuous curves and not discrete points, in contrast to the traditional "electron swarm" approaches. The dependences of the momentum transfer cross sections and the first two scattering phases are obtained for five noble gases in the energy range from 0.01 to 1 eV. In this energy range there are no irregularities in the energy dependence of the momentum transfer cross section, apart from the Ramsauer effect in Ar, Kr, and Xe. The scattering lengths found by this method are 1.17, 0.204, − 1.55, − 3.50, and − 6.50 a.u. for helium, neon, argon, krypton, an xenon, respectively.

PACS numbers: 34.80.Dp

1. INTRODUCTION

Electron–atom collisions at energies less than the electron excitation energy have been attracting interest continuously for the last few decades. This interest arises from the fact that low-energy collisions occur without any strong distortion of the atomic structure and, therefore, information on the scattering process can be used to obtain a better understanding of the structure of the inner and outer induced and unperturbed atomic fields.

There are two experimental approaches to the problem of elastic electron–atom collisions: the beam method and the electron swarm method. The former was first proposed and used by Ramsauer and Kollath[1,2] and it led to the discovery of a strong irregularity in the energy dependences of the elastic scattering cross sections $\sigma_m(w)$ of heavy noble gases at energies amounting to a few tenths of an electron-volt. The beam method has a number of advantages (high resolution, direct determination of the cross sections, etc.), but it is not very suitable for the study of collisions at energies $w < 0.1$ eV, since it is hardly possible to generate a monokinetic electron beam of acceptable intensity with this energy. Moreover, the pressures required in this case (10^{-2}–10^{-3} Torr) cannot be determined by modern instruments with satisfactory precision and this gives rise to an error in the cross sections which is far too high. The other experimental approach, i.e., the electron swarm method,[3] is based on reconstruction of the dependence $\sigma_m(w)$ from the electron transport coefficients (mobility, diffusion coefficient, effective collision frequency) in a gas discharge or, more frequently, in an afterglow plasma. The experiments involved probing of a plasma by an electro-static field in order to determine the mobility or the diffusion coefficient, and the technique is usually called the dc electron swarm method.[4] The effective collision frequency is usually determined by microwave probing of a plasma, which gives the active part of the admittance related to the effective collision frequency, which is then used to find the elastic scattering cross section $\sigma_m(w)$. This type of experiment is known as the ac electron swarm method.[5,6]

In all cases the function $\sigma_m(w)$ used in the electron swarm experiments is replaced by an average value within the limits of the thermal scatter. This makes it possible to probe a certain range of energies by varying the electron temperature T_e and taking the cross sections averaged in the limits of the thermal scatter as exact at the energy equal to kT_e (k is the Boltzmann constant). A numerical analysis, involving selection of numerical values of the cross sections giving the best agreement between the results of kinetic calculations of the transport coefficients and the measured values, was developed by Frost and Phelps[7] for the dc electron swarm method and was later modified for the ac method.[8,9] The method of Frost and Phelps has given the best results obtained so far. However, it suffers from a number of shortcomings. In particular, the minimum energy at which measurements of σ_m can be made is kT (where T is the gas temperature), so that the cryogenic technique is needed in the range $w < 0.1$ eV and even then the lowest energy is 1×10^{-3} eV. Moreover, the results of measurements are the average values, which makes it difficult to detect a possible fine structure in the dependence $\sigma_m(w)$. Finally, each cycle of measurements subjected to a numerical analysis gives one discrete point for σ_m, which reduces the accuracy of the results since it is extremely difficult to maintain the experimental conditions absolutely the same from one cycle to another. Moreover, plotting of the $\sigma_m(w)$ curve point by point makes the task of detecting fine effects practically hopeless.

It is worth noting particularly the suggestions to use electron cyclotron resonance (ECR) in a weakly ionized plasma to study electron–atom collisions. The first such suggestion was made by Kelly, Margenau, and Brown,[10] who showed that the half-width of the ECR

 0038-5646/81/061153-06$02.40

line is equal to the effective collision frequency if $\sigma(v) = \text{const}/v$, so that in some cases one can find the value of σ_m. Another suggestion to use ECR in studies of the collision cross sections was made by Rokhlenko,[11] who showed that in the case of sufficiently strong irregularities of the function $\sigma_m(w)$ one may observe splitting of an ECR line into doublets and triplets. This itself can be used as a method of identifying strong irregularities of the cross section[1)] when (as stated by the author) a probing microwave field heats considerably the plasma electrons.

We shall propose a method (ECR spectroscopy) which is largely free of the shortcomings of the familiar electron swarm method and which imposes no special conditions on the function $\sigma_m(w)$ and does not require continuous perturbation of the electron distribution function. The method does not involve averaging over an energy interval (although probing of a neutral gas is performed using a swarm of electrons of temperature T_e) and it makes it possible to carry out just one cycle of measurements lasting a few seconds and thus obtain a continuous $\sigma_m(w)$ curve covering several orders of magnitude of w by a computer analysis of the results. The lower limit on the energy scale is then much less than kT.

2. ELECTRON CYCLOTRON RESONANCE SPECTROSCOPY

Information on $\sigma_m(w)$ is found by the ECR spectroscopy method from all the points on an ECR absorption curve (or on a finite part of this curve) recorded in an afterglow plasma. The ECR spectrum obtained for a constant amplitude of an electric field E in a probing microwave of angular frequency ω applied to a weakly ionized magnetoactive ($\nu^2 \ll \omega^2$) plasma is described by a dependence of the active conductance $\Sigma_\perp^{(a)}$ transverse to a magnetic field on the detuning $\Omega = \omega - \omega_c$ from the resonance, where $\omega_c = eB/mc$ and B is the magnetostatic field induction ($E \perp B$), as given in Ref. 12:

$$\Sigma_\perp^{(a)}(\Omega) = \varkappa \int_0^\infty R v v^3 (\partial f_0/\partial v)\, dv; \tag{1}$$

$$R = (\nu^2+\Omega^2)^{-1}, \tag{2}$$

$$\nu = N v \sigma_m. \tag{3}$$

Here, $\varkappa = -2\pi e^2 n/3m$, n is the electron density, N is the concentration of atoms, and v is the electron velocity.

The symmetric part of the distribution function $f_0(v, \Omega)$ was found for this case by Kelly, Margenau, and Brown[10] in the form

$$f_0(v, \Omega) = \beta \exp\left\{-\int_0^v \frac{mv\,dv}{kT + e^2E^2R/6m\chi}\right\}, \tag{4}$$

where $\chi = 2m/M$ (in the absence of inelastic collisions), β is a normalization constant, and M is the mass of an atom.

The expressions (1)–(4) allow us to obtain working formulas used in the method of ECR spectroscopy of a plasma in which all collisions are elastic:

$$f_0(w, \Omega) = \beta \exp\left\{-\int_0^w \frac{dw}{kT + \nu\tau_h e^2E^2/6m(\nu^2+\Omega^2)}\right\}, \tag{5}$$

$$S(\Omega) = \Gamma \int_0^\infty \frac{w^{1/2} f_0(w)\, dw}{6mkT(\nu+\Omega^2/\nu)/e^2E^2 + \tau_h}. \tag{6}$$

Here, Γ is a normalization constant ensuring that $S(0) = 1$; $S(\Omega)$ is a normalized ECR absorption spectrum; $w = mv^2/2$ is the electron energy; $\tau_h = (\chi\nu)^{-1}$ is the characteristic electron heating time when a high-frequency field acts continuously on a plasma. If this field is in the form of pulses of duration τ_p, Eqs. (5) and (6) remain valid only in the case of sufficiently long pulses when $\tau_p > \tau_h$. In the opposite case, i.e., when $\tau_p > \tau_h$, Eqs. (5) and (6) should be modified by replacing τ_h with τ_p (Ref. 13).

Under given experimental conditions (E, N, M, τ_p), the distribution function (4) can be calculated using Eq. (3) and this can be done for any value of the detuning Ω and any specified model function $\sigma_m(w)$. Substitution of the calculated function $f_0(w, \Omega)$ into Eq. (6) makes it possible to calculate for the same model dependence $\sigma_m(w)$ the form of the spectrum $S(\Omega)$. The function $S(\Omega)$ found in this way can be compared with the experimental curve. Selecting the model functions $\sigma_m(w)$ and comparing the corresponding functions $S(\Omega)$ with the measured ECR spectra, we can find a model function that ensures the agreement between the simulated ECR spectrum and that found experimentally within the specified limits of precision. In this case the model curve describes with appropriate precision the required dependence $\sigma_m(w)$. This procedure allows us to determine, in principle, the function $\sigma_m(w)$ with any arbitrarily high precision, limited only by the experimental error in the determination of the ECR curve.

The model functions can, in principle, be selected in any form. However, we shall prefer to use the model functions $\sigma_m(w)$ in the form given by the modified theory of atomic radius developed by O'Malley, Rosenberg, and Spruch[14] and based on the expansion of the elastic scattering cross section in terms of partial waves.[15] For low energies, O'Malley[16] proposed an expression for the expansions of the cross section and scattering phases used by us as the model functions with three fitting parameters:

$$\sigma_m = 4\pi \sum_{L=0}^{3} (\eta_L/q - \eta_{L+1}/q)^2 (L+1); \tag{7}$$

where

$$\left.\begin{aligned} \eta_0/q &= -A - 0.2839\alpha w^{1/2} - 0{,}0490 A\alpha w \ln w + Bw, \\ \eta_1/q &= 0.05679\alpha w^{1/2} - 0.07353 Cw; \\ \eta_L/q &= 0.85175 w^{1/2}/[(2L+3)(2L+1)(2L-1)] \\ &\quad \text{for } L = 2,\ 3,\ 4. \end{aligned}\right\} \tag{8}$$

Here, η_L are the scattering phases in radians; $q = (2mw)^{1/2}/\hbar$ is the de Broglie wave number of an electron in units of a_0^{-1}; a_0 is the Bohr radius; α is the polarizability in units of a_0^3; A is a fitting parameter (scattering length) in units of a_0; B and C are fitting parameters in units of a_0^3; the electron energy (in electron-volts) is also expressed in terms of a_0 using $w\ [\text{eV}] = 13.6(a_0 q)^2$ (Ref. 17). The usual values were assumed for the polarizabilities: 1.36 for helium, 2.65 for neon, 11.0 for argon, 16.6 for krypton, and 27.0 for xenon.[18]

3. EXPERIMENTS AND ANALYSIS OF RESULTS

The purpose of our experiments was to record the ECR spectra of noble gases at $T_e = T = 300°K$ and to determine as accurately as possible the values of E, Ω, and N under conditions such that all the factors influencing the ECR spectrum could be ignored compared with the contribution of elastic electron–atom collisions.

The experiments involved continuous recording of the intensity of a microwave signal transmitted by a resonator in which a small part was occupied by a magnetoactive weakly ionized plasma resulting from afterglow; at the same time the magnetic field was varied slowly in the vicinity of the value corresponding to the exact resonance. The measurements were carried out during the late stages of afterglow in He, Ne, Ar, Kr, and Xe when the plasma could be regarded quite accurately as in equilibrium with a temperature equal to the temperature of the walls of the discharge tube (300°K).

The main parameters of these experiments were as follows: the wavelength of the probing microwave signal was $\lambda = 3.04$ cm ($\omega = 6.20 \times 10^{10}$ rad/sec); the probing signal power was $\leqslant 1 \times 10^{-3}$ W; the duration of the probing pulses was $\tau_p \leqslant 0.3$–3.0 μsec; the magnetic meter was 6 mm; the plasma length was 40 mm; the part of the plasma used directly for the measurements was 7 mm long; the neutral gas pressure was 1.0–10 Torr; the duration and repetition frequency of the ionizing pulses were 10 μsec and 1 kHz; the delay of the probing pulses was 0–800 μsec.

We used the apparatus shown schematically in Fig. 1. A rectangular resonator excited at the TE_{101} mode (21 ×70×21 mm) was placed between the poles of a permanent magnet. A glass discharge tube passed through the resonator in such a way that its axis coincided with the direction of the magnetic field and it was connected to a vacuum system. The gas inside the tube was ionized by periodic high-frequency pulses from a 40 W generator operating at a carrier frequency of 40 MHz.

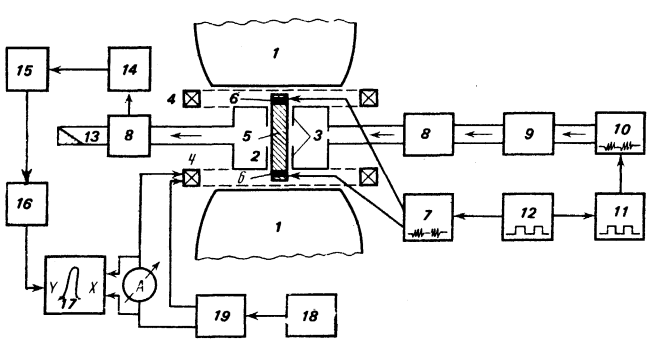

FIG. 1. Block diagram of the apparatus: 1) poles of a permanent magnet; 2) resonator; 3) metal flanges; 4) magnetic scanning coils; 5) discharge tubes; 6) ring electrodes for discharge excitation; 7) high-frequency generator of discharge excitation; 8) measuring line; 9) isolator valve; 10) measuring microwave oscillator; 11) generator of delayed pulses; 12) synchronizing generator; 13) matched load; 14) detector; 15) integrating unit; 16) dc amplifier; 17) X–Y plotter; 18) ac voltage regulator; 19) stabilized rectifier for scanning coils.

Special metal flanges were placed inside the resonator and these limited the active volume of the plasma to a few millimeters around the geometric center of the resonator; this measure ensured a sufficient homogeneity of the fields E and B in the region subjected to probing. A pair of thin coils, coaxial with the main field and forming a Helmholtz system, provided magnetic scanning.

The apparatus was operated as follows. A synchronizing generator triggered periodically the ionizing pulse generator and, after a controlled delay time, a generator of probing pulses. These pulses passed through an isolator and a measuring line; they then passed through a waveguide and entered the resonator through an optimizing slit. The microwave pulses transmitted by the resonator and a second measuring line entered the final absorbing load. The microwave signal transmitted by the resonator was measured with a square-law crystal detector. The crystal in this detector produced periodic pulses whose amplitude was proportional to the microwave power absorbed by the plasma for a given detuning and a given delay of the probing pulse. Continuous recording of the detector pulse amplitude as a function of the current in the magnetic scanning coils gave the ECR spectrum.

The procedure of numerical simulation of the ECR spectrum was as follows.

An experimental ECR absorption curve (one half the curve) was introduced in the form of twenty points corresponding to twenty values of the detuning. In principle, the number of such points could be increased to any value. The fitting parameters were first assumed to be $A^{(0)} = B^{(0)} = C^{(0)} = 1$ and the function $\sigma_m^{(0)}(w)$ was calculated; then, the distribution function and the corresponding point on the curve simulating the ECR spectrum were computed for each of the twenty detunings. Next, for each detuning the deviation of the simulating ECR curve from the experimental results was found. When the sum of the squares of these deviations exceeded a specified value, the fitting parameters were corrected by one step and the cycle was repeated. When the simulating and experimental curves were sufficiently close, the final results were plotted as the values of the cross sections, the experimental and simulating ECR spectra, and the energy distribution functions for each of the twenty detunings. The values of the fitting parameters and of the total rms error were printed in a numerical form.

4. RESULTS

Figure 2 shows the experimental and simulating ECR spectra obtained for five noble gases. The selection of the values of E, N, and τ_p for each gas was governed by the need to satisfy the conditions of validity of the working formulas (5) and (6). The simulating spectra were obtained after 150–200 fitting cycles in which all three parameters were varied. The corresponding $\sigma_m(w)$ functions are plotted in Fig. 3. It is interesting to note that although the ECR spectra of all five gases do not have any clear irregularities, the functions $\sigma_m(w)$ are very different. First of all, we can see from

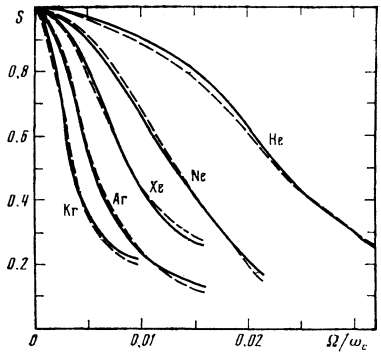

FIG. 2. Experimental (continuous) and simulating (dashed) ECR absorption spectra obtained for various parameters (μ is the number of numerical simulation cycles). He: $N = 3.30 \times 10^{16}$ cm^{-3}, $E = 1.2$ V/cm, $\tau_p = 3$ μsec, $T_e = 300$ °K, $\mu = 116$. Ne: $N = 1.65 \times 10^{17}$ cm^{-3}, $E = 1.2$ V/cm, $\tau_p = 0.6$ μsec, $T_e = 300$ °K, $\mu = 130$. Ar: $N = 3.30 \times 10^{17}$ cm^{-3}, $E = 1.2$ V/cm, $\tau_p = 0.3$ μsec, $T_e = 300$ °K, $\mu = 148$. Kr: $N = 0.98 \times 10^{17}$ cm^{-3}, $E = 0.9$ V/cm, $\tau_p = 0.4$ μsec, $T_e = 300$ °K, $\mu = 153$. Xe: $N = 3.30 \times 10^{16}$ cm^{-3}, $E = 1.2$ V/cm, $\tau_p = 0.4$ μsec, $T_e = 300$ °K, $\mu = 161$.

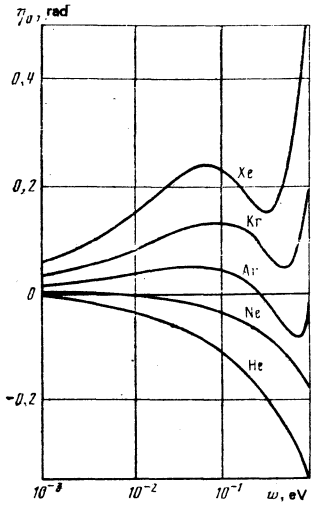

FIG. 4. Zeroth scattering phases plotted as a function of the energy for five noble gases, corresponding to the simulating spectra in Fig. 2.

Fig. 3 that the heavy gases exhibit the Ramsauer effect, but this is not true of He and Ne. Another feature of the curves in Fig. 3 is the fact that the scattering cross section for helium is almost independent of the energy in the range 10^{-3}–1 eV. Finally, the third remarkable property is the exceptionally small scattering cross section of neon at subthermal energies.

Figure 4 shows the dependences of the zero scattering phase η_0 (representing the head-on collisions) for all five rare gases. It is worth noting the presence of extrema in the Ramsauer gases and their absence in the case of He and Ne.

Finally, Fig. 5 shows the energy dependences of the first scattering phase η_1 obtained for the investigated gases. Like the zeroth phases, the heavy gases again exhibit rapid changes near the energies corresponding to the Ramsauer minimum, whereas the curves obtained for the light gases are completely smooth.

5. PRECISION AND RELIABILITY

If all the factors (apart from elastic collisions) affecting the ECR spectrum are eliminated and the gas density is sufficiently low for the collisions to be essentially binary, the absolutely correct ECR curve recorded for $0 \leq \Omega \to \infty$ and simulated with absolute precision gives the function $\sigma_m(w)$ which is perfectly accurate right down to $w = 0$. However, in practice there is no need to record the resonance curve for $0 \leq \Omega \to \infty$ because, strictly speaking, any finite part of the ECR curve contains integral information on the cross sections at any energy (apart from those, naturally, which correspond to inelastic scattering). Therefore, in our experiments the ECR absorption curve was recorded only in the range of Ω where the resonance was strong, i.e., in the range of detunings corresponding to two or three half-widths of the resonance curve.

Nevertheless, in spite of the fact that particles of any (including infinitesimally low) energy can participate in the ECR absorption process, the results obtained can be regarded as acceptably accurate only down to energies such that the total number of particles is sufficiently large compared with the number which have the average energy.

In fact, each point on the resonance curve corresponds to integral absorption and the contribution of

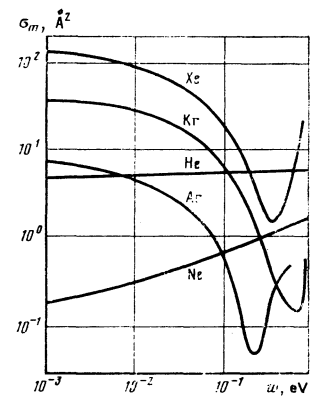

FIG. 3. Elastic scattering cross sections plotted as a function of the energy for five noble gases, corresponding to the simulating spectra in Fig. 2.

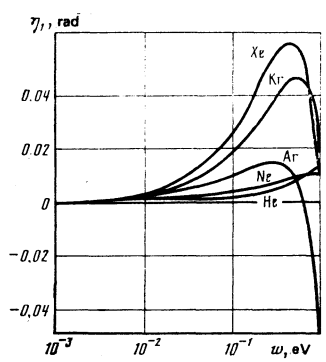

FIG. 5. First scattering phases plotted as a function of the energy for five noble gases, corresponding to the simulating spectra in Fig. 2.

particles of given energy to this absorption increases on increase in the density of particles of this energy in the phase space. Therefore, the results can be regarded as reliable with a given accuracy only up to the energies which correspond to the values of the energy distribution function representing a significant proportion of the maximum of this function. For example, in the case of a Maxwellian distribution and a negligible error in the experimental ECR curve, we find that if the simulation is accurate to within 5% at any point when $T = 300°K$, sufficient sensitivity of the ECR spectroscopy method can be ensured at low energies down to 1×10^{-3} eV. Cryogenic technique and very weak probing fields should make it possible to go down to 5×10^{-6} eV.

On the basis of the above discussion and bearing in mind the errors in the experimental parameters and in the simulation procedure, we estimated the error in the dependences $\sigma_m(w)$ obtained for all the investigated gases and this was within 10% in the energy range 0.001–1 eV.

The uniqueness of the numerical values of $\sigma_m(w)$ could not be guaranteed, as in any other case when integral relations are used. However, in the case of the ECR spectroscopy method there is another factor which—in our opinion—limits greatly the number of possible solutions and may give a unique solution. This factor is that the fitting in the ECR spectroscopy method is made not to a single experimental point (as , for example, in the case of discrete measurements of the transport coefficients) but simultaneously for a set of points representing a continuous curve. The required solution is then automatically subject to the condition that the fitting parameters should remain constant for all the points of this curve and for any part of the curve.

This naturally cannot be regarded as proof of the uniqueness of our results, but since the same values are obtained for different starting values of the fitting parameters (as found by us), we may assume that the functions $\sigma_m(w)$ obtained above are satisfactory.

6. DISCUSSION

One of the main results of the present study is that the experimental ECR spectra of five noble gases can be simulated with satisfactory precision on the basis of the modified theory of the effective radius. This means that the concepts of this theory are supported by the experimental results and that the fitting parameters can be used to obtain quantitative information on the scattering of electrons by atoms. Let us consider the parameter A which determines the zeroth scattering phase at subthermal energies.

The absolute value of the parameter A (scattering length) is the equivalent radius of the scattering potential of an atom (including the polarization, internal electrostatic, and exchange potentials) when the initial energy of an electron is infinitesimally small. The sign of the scattering length represents the effective (integral) sign of the scattering potential. The positive

TABLE I. Scattering lengths for noble gas atoms (in units of a_0).

Method	Reference	He	Ne	Ar	Kr	Xe
ECR spectroscopy	Our results	1.17	0.204	−1.55	−3.50	−6.50
Extrapolation of results of beam experiments	[16]	1.19	0.24	−1.70	−3.70	−6.50
DC electron swarm	[19, 20]	1.15	–	−1.69	−3.20	−6.00
	[21]	1.19	–	−1.31	−2.80	−5.35
AC electron swarm	[22]	1.14	0.39	–	−3.20	−5.60
	[23]	–	–	−1.50	–	–
Theory	[24]	1.46	–	–	–	–
	[25]	–	0.347	−1.60	–	–

scattering lengths correspond to the effective repulsive potential, whereas the negative lengths correspond to the attractive potential. Table I gives the numerical values of the scattering lengths in atomic units found in the present study, and also in other experiments and theoretical treatments.[2)]

It is clear from Table I that the effective scattering potential at very low energies changes qualitatively from the repulsive for the light noble gases to the attractive for the heavy gases. The scattering potential of the neon atoms corresponds to the region where the scattering length passes through zero. The small positive value of the scattering length of neon means that the neon atoms are "seen" by low-energy electrons as representing overall weakly repulsive scattering centers, which should make the neon gas highly transparent to electrons of near-zero energies, compared with other rare gases, including helium. On this basis we can expect an exceptionally high mobility of excess electrons in liquid neon. The physical reasons for this special behavior of neon are as follows.

The integrated effect of the scattering of an electron by an atom is governed by the deflecting action of all types of the interaction potential, namely the long-range polarization potential and short-range potentials, specifically the screened electrostatic potential of the nucleus and the exchange potential. Since the polarization potential of an atom is induced by the incident electron itself and is related to changes in the electron shells of the atom, the scattering effect of this potential depends on the flight time of the electron pass the atom (i.e., on the electron energy) and it decreases when the energy is increased. The exchange potential of rare gas atoms is repulsive (because of the Pauli principle) and, in the first approximation, it is independent of the electron energy. Thus, around a certain specific energy, depending on the static polarizability of a given atom, the attractive effect of the polarization potential (and of the internal electrostatic potential) may be compensated by the repulsive effect of the exchange potential, so that the net scattering effect is small. In the heavy gases with a high polarizability this compensation should obviously occur at higher energies than in the light gases and this is manifested by the Ramsauer effect. In the case of the light atoms, such as those of helium which has a very low polarizability, such compensation cannot occur even at zero energy. Neon occupies an intermediate position when the polarization effect is almost compensated by the exchange effect near zero energy. In this sense, we

can conclude nominally that neon exhibits also the Ramsauer effect but at an energy close to zero. The positive value of the scattering length of neon indicates that the hypothetical Ramsauer minimum of neon is not attained even at zero energy, but the scattering cross section is close to the Ramsauer value.

7. CONCLUSIONS

The ECR spectroscopy method is an effective means for investigating electron–atom collisions and it is largely free of the known shortcomings of the traditional approaches. In principle, the varous energy intervals can be investigated with a very high precision if the electron temperature is selected so that the maximum of the distribution function coincides with the middle of the investigated energy interval. This makes it possible to carry out measurements not only over a wide range of energies but also to obtain detailed information in narrow energy intervals.

The results obtained for all five noble gases can be made even more accurate, but a comparison with those obtained by other methods shows that they are satisfactory. In principle, the ECR spectroscopy method can be extended to the case of inelastic collisions in both atomic and molecular gases. However, one would then have to modify Eq. (4), which should allow for the inelastic processes.

The authors are grateful to B. M. Smirnov for discussing this investigation.

[1)]We shall show later that irregularities such as the Ramsauer effect are not sufficiently strong to cause splitting of the type predicted by Rokhlenko.

[2)]After the present paper was completed, the authors became aware of the recent work of O'Malley and Crompton[26] where the drift velocities were used to find the scattering length in neon amounting to 0.214.

[1]C. Ramsauer and R. Kollath, Ann. Phys. (Leipzig) **3**, 536 (1929).
[2]C. Ramsauer and R. Kollath, Ann. Phys. (Leipzig) **12**, 529 (1932).
[3]L. G. Huxley and R. W. Crompton, The Diffusion and Drift of Electrons in Gases, Wiley, New York, 1974.
[4]A. G. Robertson, J. Phys. B **5**, 648 (1972).
[5]A. L. Gilardini and S. C. Brown, Phys. Rev. **105**, 31 (1957).
[6]C. L. Chen, Phys. Rev. **131**, 2550 (1963).
[7]L. S. Frost and A. V. Phelps, Phys. Rev. **127**, 1621 (1962).
[8]C. R. Hoffmann and H. M. Skarsgard, Phys. Rev. **178**, 168 (1969).
[9]C. Sol, F. Devos, and J. C. Gauthier, Phys. Rev. A **12**, 502 (1975).
[10]D. C. Kelly, H. Margenau, and S. C. Brown, Phys. Rev. **108**, 1367 (1957).
[11]A. V. Rokhlenko, Zh. Eksp. Teor. Fiz. **69**, 169 (1975) [Sov. Phys. JETP **42**, 87 (1975)].
[12]W. P. Allis, in: Handbuch der Physik (ed. by S. Flügge), Vol. **21**, Springer Verlag, Berlin, 1956, p. 383.
[13]V. E. Golant, Sverkhvysokochastotnye metody issledovaniya plazmy (Microwave Methods for Plasma Investigation), Nauka, M., 1968.
[14]T. F. O'Malley, L. Rosenberg, and L. Spruch, Phys. Rev. **125**, 1300 (1962).
[15]J. C. Bowe, Phys. Rev. **117**, 1416 (1960).
[16]T. F. O'Malley, Phys. Rev. **130**, 1020 (1963).
[17]D. E. Golden, Phys. Rev. **151**, 48 (1966).
[18]J. H. Van Vleck, The Theory of Electric and Magnetic Susceptibilities, Clarendon Press, Oxford, 1932.
[19]J. L. Pack and A. V. Phelps, Phys. Rev. **121**, 798 (1961).
[20]J. L. Pack, R. E. Voshall, and A. V. Phelps, Phys. Rev. **127**, 2084 (1962).
[21]L. S. Frost and A. V. Phelps, Phys. Rev. A **136**, 1538 (1964).
[22]A. V. Phelps, O. T. Fundingsland, and S. C. Brown, Phys. Rev. **84**, 559 (1951).
[23]H. B. Milloy, R. W. Crompton, J. A. Rees, and A. G. Robertson, Aust. J. Phys. **30**, 61 (1977).
[24]R. W. LaBahn and J. Callaway, Phys. Rev. A **135**, 1539 (1964).
[25]D. G. Thompson, Proc. R. Soc. London Ser. A **294**, 160 (1966).
[26]T. F. O'Malley and R. W. Crompton, J. Phys. B **13**, 3451 (1980).

Translated by A. Tybulewicz